

A Remarkable Example of Bubble Nucleation Suppression

J. CREECH, V. DIVINO, W. PATTERSON, P.J. ZALESKY*and C.E.BRENNEN†

Abstract

Suppression of cavitation is a relatively common goal of fluid engineers and therefore examples of bubble nucleation suppression in other technological contexts are useful in suggesting ways in which such suppression might be achieved. In this paper we describe a remarkable example of bubble nucleation suppression achieved by a combination of the elimination of nucleation sites and the reduction of bubble growth time. The context is the invention of a device that allows the injection of aqueous solutions highly supersaturated with oxygen into the bloodstream without the formation of significant gaseous oxygen bubbles.

Key Words: Nucleation, suppression, supersaturated oxygen solution injection, bloodstream.

1. Introduction

This paper describes a remarkable example of bubble nucleation suppression. The context is a device for the rapid delivery of large quantities of dissolved oxygen to the bloodstream without the formation of oxygen gas bubbles. The potential medical benefits of a successful strategy of this kind are substantial and multi-faceted. Deprivation of oxygen even for brief periods of time such as occur during heart attacks or strokes results in cell damage or death - and is the primary cause of permanent physiological damage during these events. Consequently rapid therapeutic oxygen delivery systems could substantially enhance the treatment, for example, of acute myocardial infarction or acute cerebral stroke. It may also find application in a broad range of other medical treatments.

The strategy discussed here has been described previously (Brereton *et al.*⁽²⁾). It involves the preparation of a highly concentrated solution of oxygen in an aqueous solution under very high pressure and the injection of this liquid into the bloodstream through a small capillary tube or tubes. The innovation is the ability to do this in a way that avoids the formation of significant or measurable gaseous oxygen bubbles either inside the capillary or in the highly supersaturated

jet that emerges from the tube. This requires two techniques. First the avoidance of nucleation within the capillary over the distal length, l , for which the liquid pressure is below the saturated pressure for the particular oxygen concentration being deployed. And, second, the avoidance of nucleation within the emerging jet. The jet mixes with the surrounding liquid and thus becomes rapidly diluted. If this mixing time is less than the time required for bubbles to grow to significant size then the objective has been achieved.

Two basic strategies mitigate for success. The first of these is to prepare and treat the interior surface of the capillary in a way that minimizes the occurrence of nucleation sites. The second of the strategies is that of high fluid velocity. Inside the capillary tube this leads to a large longitudinal pressure gradient which implies a short distal length of tube for which the fluid pressure is below the saturation pressure. Minimizing the interior surface area below the saturation pressure minimizes the chance of a nucleation site being activated. A second benefit of high fluid velocity is that it maximizes the rate of mixing in the jet external to the capillary.

2. Nucleation Sites

In aqueous solutions at normal temperatures, it has been well established⁽³⁾ that nucleation begins with small, micron-sized crevices in the solid surface in contact with the liquid, a process known as heterogeneous nucleation. This is distinct from homogeneous nucleation which refers to the formation of bubbles in the body of a pure liquid as a result of thermodynamic fluctuations. The fact that heterogeneous nucleation dominates in aqueous liquids at normal temperatures, is simply a reflection of the fact that an applied tension will activate far more heterogeneous sites than homogeneous sites.

In the context of the present devices, Brereton *et al.*⁽²⁾ theoretically explored the possibility of homogeneous nucleation. Subsequently, it became clear⁽¹⁾ that treatment of the interior surface of the capillary tubes had such a radical effect on the nucleation phenomenon that heterogeneous surface nucleation rather than homogeneous nucleation was clearly the dominant phenomenon. The current paper describes some

*TherOx, Inc., Irvine, CA 92612, USA

†California Institute of Technology, Pasadena, CA 91125, USA

of those experimental observations and the conclusions to be drawn from them.

3. Modelling Nucleation

Creech *et al.*⁽¹⁾ describe a fluid mechanical model of the nucleation potential in these flows and we provide a brief summary here. A key feature is the pressure difference or “tension” which motivates nucleation in the distal end of the capillary (internal diameter, d). The tension, $p_{ssat} - p$, is defined as the difference between saturation pressure, p_{ssat} , and the local liquid pressure, p , in the capillary. Under flowing conditions this increases linearly with distance, x , along the tube from zero at the critical location where $p = p_{ssat}$ (called the “saturation location”) to $p_{ssat} - p_e$, at the distal end of the capillary, p_e being the ambient pressure at the capillary exit. Since most of the capillary tube flows considered here have Reynolds numbers, Re_t (defined as $\rho_l V d / \mu$ where V is the volumetric mean velocity of the flow and ρ_l and μ are the liquid density and dynamic viscosity) that cause the flow to be in the laminar regime, it follows that the distance, l , from the saturation location, $x = 0$, to the end of the capillary, $x = l$, is given by

$$l = \frac{(p_{ssat} - p_e)d^2}{32\mu V} \quad (1)$$

Note that in a $100\mu m$ tube at a velocity of $4m/s$ and an exit tension of $5MPa$ (a typical Brereton *et al.*⁽²⁾ data point) the length l is $0.39m$.

Creech *et al.*⁽¹⁾ then consider a nucleation site on the interior surface of the distal end of the capillary. A bubble grows attached to this site due to diffusion of gas from the liquid into the bubble. When it reaches some critical size, the forces due to the flow around the bubble exceed the surface tension forces holding the bubble in place, the bubble breaks off and is swept out of the capillary. The nucleation site is characterized by a size R_i because it begins to produce growing, visible bubbles when the tension exceeds the restraining surface tension pressure, $2S/R_i$ (where S is the surface tension). Therefore, only those sites larger than a critical size, $R_{ic}(x)$, will be activated (produce bubbles) at the location, x , where

$$R_{ic}(x) = \frac{Sd^2}{16\mu V x} = \frac{2S}{(p_{ssat} - p_e)(x/l)} \quad (2)$$

and only those nucleation sites larger than $Sd^2/16\mu V l = 2S/(p_{ssat} - p_e)$ get activated anywhere within the capillary. A few numbers provide guidance on the magnitude of R_{ic} in the present context. For a $d = 100\mu m$ capillary tube at $V = 4m/s$ and $(p_{ssat} - p_e) = 5MPa$ the values of R_{ic} at $x/l = 0.25, 0.5$ and 0.75 are respectively $0.112\mu m,$

$0.056\mu m$ and $0.028\mu m$. These are very small nucleation sites and some may be too small to produce exit bubbles of observable size.

By considering the mass transport of oxygen into the attached bubble, Creech *et al.*⁽¹⁾ arrive at a bubble growth rate that leads to a bubble size, $R(t)$, given by

$$R = C^{**}(DV)^{\frac{1}{3}} \left\{ \frac{\rho_l(p_{ssat} - p)t}{H\rho_g} \right\}^{\frac{2}{3}} \quad (3)$$

where C^{**} is a constant of order unity, D is the mass diffusivity of the dissolved gas in the liquid (D values for O_2 and CO_2 in water are $2.07 \times 10^{-9}m^2/s$ and $1.75 \times 10^{-9}m^2/s$ respectively⁽⁴⁾), H is Henry’s Law constant defined as the saturation pressure, p_{ssat} , divided by the saturated mass concentration and ρ_g is the density of the gas at the local pressure, p .

The bubble growth phase will end when the bubble detaches from the site. Creech *et al.*⁽¹⁾ determine the departure radius, R_d , which can approach the radius of the tube, $d/2$. Combining this expression for R_d with equation 3 completes the model of the bubble growth and departure from a nucleation site at a location, x , in the capillary. Then, the frequency, f , of bubble production from a site close to the distal end of the capillary (where $p \approx p_e$ and ρ_g is the gas density outside the capillary) would be given by

$$f = CR_d^{-\frac{3}{2}}(DV)^{\frac{1}{2}} \left\{ \frac{\rho_l(p_{ssat} - p_e)}{H\rho_g} \right\} \quad (4)$$

where C is some other constant of order unity.

Creech *et al.*⁽¹⁾ also examine the growth of bubbles in the expanding jet issuing from the capillary.

5. Experiments

5.1 Equipment

A set of experiments was conducted to investigate the onset of nucleation in highly super-saturated liquid jets emerging from small capillary tubes. The results showed clearly that the condition of the interior surface near the exit from the capillary is a critical factor in the resulting behavior. Consequently the material of the capillary, its roughness, coating(s) and preparation were important. The experiments reported here focussed on drawn silica capillaries with internal diameters ranging from $75\mu m$ to $325\mu m$ though results are also described for some polymer (PEEK and Teflon) capillaries. The silica capillaries were cleaved in such a way that the end appeared very rectangular and flat under microscopic examination. Some which showed significant deformity or irregularity were discarded. On the other hand the PEEK capillaries were sliced with sharp razor while being held in a jig.

The interior surface of the silica capillaries were prepared in various ways. Some of the capillaries were

coated with benzalkonium heparin (BKH for short), a biocompatible treatment designed for medical devices. After pre-treating the surface with ethanol, the BKH was laid down in a 10% solution in isopropyl alcohol (aka 2-propanol). The capillary was allowed to dry as the alcohol evaporated.

The experiments utilized various concentrations of oxygen and carbon dioxide in distilled water (filtered down to $2\mu m$) at normal temperatures. These solutions were prepared under high pressure so that the saturated pressures of oxygen employed varied from 0.17 to 6.41MPa though the focus was on the higher levels above 1.38MPa. Experiments were also conducted with carbon dioxide because its much higher solubility would provide information on the importance of that parameter; CO_2 saturated pressures ranging from 0.41 to 3.37MPa were employed. Note that the Henry's Law constants, H , for oxygen and carbon dioxide in water at $25^\circ C$ are 2590MPa and 70MPa respectively⁽⁶⁾. For later reference we also note that the same properties for ethanol rather than water are much smaller being 249MPa and 17MPa respectively⁽⁵⁾.

The experiments themselves were simple. Using a special high pressure delivery system (US Patent 5,893,838) in which the flow rate could be carefully adjusted, the highly concentrated solutions were pumped through the capillary tube whose distal end was submerged in a large beaker of water (large so that dissolved gas build up did not result in nucleation in the host liquid). Careful visual observation of the emerging jet determined whether or not nucleation was occurring. Sometimes a microscope was used to aid these observations.

5.2 Jet Visualization

The experiments showed that whether the flow within the capillary tube was laminar or turbulent could have a significant impact on whether or not nucleation occurred. The usual Reynolds numbers for transition in a tube range from 2000 to 4000 with rougher tubes having lower values. In the current experiments this transition could be readily investigated by using alcohol rather than water as the host liquid in the receiving beaker so that the emerging jet could be readily visualized.

At low Reynolds numbers when the flow within the capillary was laminar, the emerging jet was smooth and grew very slowly with distance from the end of the capillary as exemplified by figure 1. This observation may be strange to those expecting instability and transition to occur just downstream of the exit. Such would indeed be the case for a jet emerging from a nozzle with a relatively uniform velocity profile and therefore a strong shear layer at the jet surface. However, these emerging velocity profiles are quite parabolic, have no concentrated shear layer and are much less

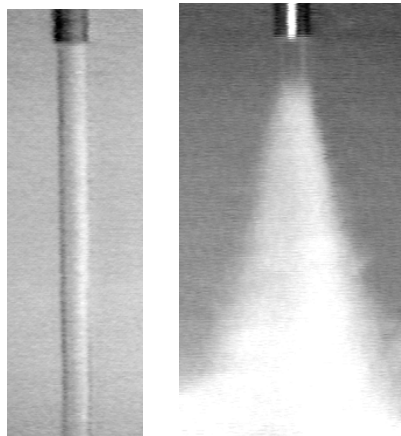


Figure 1: Frames from a normal video showing typical laminar (left) and turbulent jets (right) emerging from a $325\mu m$ capillary.

unstable. Other capillaries (particularly the rougher PEEK capillaries) did show transition to turbulence though typically 10 to 15 jet diameters from the exit.

Irrespective of the nature of the jet, it was clear that, above some Reynolds number, the flow within the capillary underwent transition and emerged as a turbulent jet. Such a case is shown in figure 1 where the spreading angle, θ , is 25° , conventional for turbulent jets. With many capillaries (but not all) this transitional process would begin with a condition in which the appearance of the jet would flip-flop back and forth between the photographs in figure 1. As the flow rate was increased, the turbulent jet configuration occurred for a greater fraction of the time until the laminar configuration ceased to appear. We note that the frequency of flip-flopping, F , when converted to a reduced frequency, Fd/V yielded values of the order of 10^{-4} .

Table I. Capillary Tubes.

Tube	d (μm)	Material	Transitional Values	
			$V(m/s)$	Re_t
B2	325	Silica	6.2	2020
C2	250	Silica	8.8	2210
H1	250	PEEK	6.8	1700
E2	100	PEEK	17-26	1700-2600

In the case of the PEEK tubes (which are hydraulically rougher than the silica tubes), the internal flow transition occurred, as expected, at lower flow rates and Reynolds numbers than in the silica capillaries as can be seen in Table. The following data demonstrates that all the transitional Reynolds numbers were in a range close to 2000:

5.3 Nucleation Observations

It is convenient to begin the nucleation results by describing a series of observations with a typical capillary. Normally, the capillaries began the tests in a dry state. Some (but not all) had been coated with BKH, then dried and stored. The experiments were then begun by connecting one end of the capillary to the high pressure supply system and submerging the other in the large beaker of distilled water. A flush of distilled water was run through the capillary in order to purge the system of trapped gas bubbles. The supply was then switched to the highly concentrated solution of O_2 or CO_2 . The initial supply pressure had previously been adjusted to produce the desired flow rate. Most often, if nucleation was going to occur it would happen almost instantaneously and persist as long as the flow continued. If nucleation did not occur immediately, the supply pressure and therefore the flow rate were sometimes raised or lowered in order to explore whether or not that change would induce nucleation.

In many of the cases when nucleation occurred, the capillary was subsequently disconnected from the supply and several *ml* of ethanol forced through it with a syringe (for convenience we refer to this as “ethanolization”). Then the capillary would be reconnected to the supply and the nucleation test repeated. In the majority of the cases in which this was done, the nucleation was completely suppressed - and the capillary would run indefinitely without nucleation. This was a most remarkable and dramatic phenomenon. Sometimes nucleation could be initiated by increasing the flow rate until the internal flow became turbulent (turbulence seemed to promote nucleation). In such cases, the nucleation would persist even when the flow rate was decreased so that the flow became laminar again. A similar regression was observed when the nucleation-free flow caused by ethanol was stopped, the capillary dried out and then reinstalled. It would then revert to its nucleation behavior prior to ethanolization. Thus, once nucleation sites became active again or were exposed to air, the benefit caused by the ethanol would disappear. However, another ethanolization would reinstitute the nucleation-free effect.

While the explanation for this remarkable effect may be tentative, it appears that, even underwater, the ethanol preferentially wets the solid surface and dislodges the tiny gas bubbles (nuclei) in the crevices that cause nucleation. In addition, the solubility of all gases in ethanol is much greater than in water so the ethanol may also be eliminating nucleation sites by dissolving the gas.

Ethanol also worked with the PEEK capillaries and the BKH coating on the silica also inhibited nucleation. Moreover, when a BKH coated capillary failed, ethanolization had the restorative effect described above. Indeed the ethanolized, BKH-coated capillaries were the most remarkable performers of

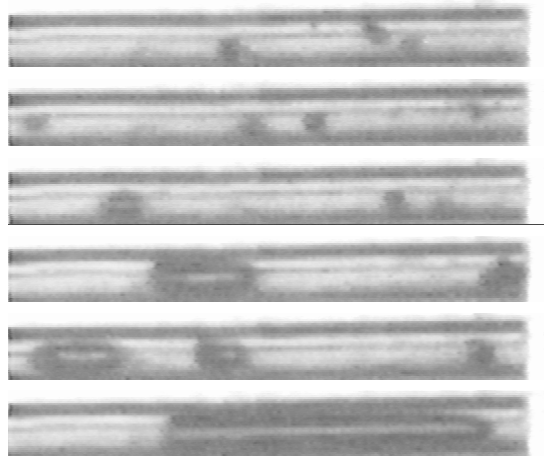


Figure 2: Six examples of high-speed video frames showing bubbles about to exit a particular $250\mu m$ capillary. The distal end of the capillary is on the right.

all. Isopropyl alcohol was also tried as an alternative to ethanol; it was less effective, working in some cases but not in others. Some nucleating capillaries could not be made non-nucleating by ethanolization but, when these were examined through the microscope, most were found to have large deformities or cracks near the distal end.

5.4 High Speed Video Observations

High-speed videos were taken of the bubbles both in the jet and in the capillary using a Redlake Imaging Motionscope 8000S video camera. At $8000fps$ it was possible to discern individual bubbles both within the capillary and in the jet. Figure 2 presents 6 examples of frames that include bubbles passing through the distal end of a $250\mu m$ BKH-coated silica capillary with a $3.45MPa$ O_2 solution flowing at $3.4m/s$. The bubbles appear as black shadows through the transparent capillary wall. The four upper frames show smaller bubbles, one of which is of the $2.5d$ variety. The lowest frame shows one of the $10d$ bubbles discussed below. High speed videos were also taken of the bubbles in the issuing jet; these showed faint images of the bubbles breaking up rapidly in the turbulent jet⁽¹⁾.

The high speed videos revealed rather different bubble production patterns in the $250\mu m$ and $325\mu m$ capillaries. We begin by detailing the observations of the bubbles emerging from a particular $250\mu m$ capillary when the flow rate was such as to produce a fluid velocity of $3.4m/s$ (figure 2). The smallest bubbles that could be observed had various globular shapes with volumetric diameters about $0.2d$. The frame-to-frame analysis suggested that these were being distorted by the flow; sometimes it appeared as though this distortion led to bubble fission since the bubble actually appeared to be a cloud of smaller bubbles. Bubbles

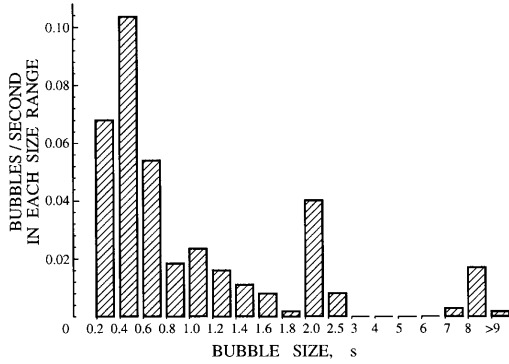


Figure 3: Typical histogram of bubble size, s , where s is 3.6 times the diameter of the bubble in mm when that diameter is less than the diameter of the tube and 3.6 times the length of the slug in mm when the length is greater than the tube diameter. This example is for the same circumstances as figure 2.

smaller than $0.1d$ may have been present in the intervening liquid but would have been difficult to resolve. However, they did not seem to be present in significant numbers or aggregate volume since the intervening liquid appeared to be clear and transparent. The largest bubbles that were observed exiting the capillary were large slugs that occupied the entire tube width and were about $10d$ long as illustrated in figure 2.

Additional observations are that a histogram of the bubble/slug size (for example, figure 3) shows that virtually all the larger slug bubbles lie within narrow size ranges. Specifically, there is a regular series of $10d$ bubbles and virtually no bubbles in the range $3d - 8d$. Another, less distinct peak occurred at $2.3d$. Second, the data showed that, after the passage of a large, $10d$ slug, there was always an extended period when no bubbles exited the capillary. In the specific case under discussion, the bubble free interval following the expulsion of a large $10d$ slug averaged $0.0018s$ in comparison with the typical interval between exiting bubbles of $0.0004s$.

Using these observations we can construct a likely course of events in the capillary. The large bubble-free interval following $10d$ slugs suggests that there is a single nucleation site quite far from the exit whose detaching bubbles regularly sweep clean all the other sites on their way to the exit. Since the subsequent bubble-free interval is $0.0018s$ and the velocity is $3.4m/s$ this implies that this particular nucleation site is at least $0.0061m$ from the exit.

Next we observe that the rate of production of $10d$ bubbles is about 160 per second. In comparison, equation 4 predicts a rate of 176 per second from a single site provided we take the reasonable value of $C = 2$. Finally, since the total number of bubbles exiting the capillary is about 2500 per second, we can estimate

(using $C = 2$) that the number of active nucleation sites in this particular capillary is 14.

But why are the large slugs $10d$ in length? This size could be the result of one or both of the following: (a) the bubble detaching from the most upstream site with a diameter of about $1d$ might collect additional gas by agglomeration with the bubbles growing at the other 14 sites and/or (b) the bubble simply expands due to the decrease in the prevailing pressure between the nucleation site and the capillary exit. However, the latter mechanism is negligible since the pressure change between the estimated site location and the exit is only about a tenth of an atmosphere. It therefore seems likely that the bubble mostly grows to $10d$ length by adding roughly $1d$ at each of the 14 sites it passes on the way to the capillary exit.

We now examine how the pattern of events changed when the flow velocity in this particular capillary was decreased from $3.4m/s$ to $1.7m/s$. At this lower velocity, the dominant large slugs were $28d$ in length rather than $10d$. Again there was a bubble-free interval following each slug but this was now $0.0035s$ (compared with the average intra-bubble spacing of $0.0009s$). However, at $1.7m/s$, this bubble-free gap again implies a nucleation site $0.006m$ upstream, in good agreement with the observation at $3.4m/s$. The production rate for the large $28d$ slugs was 115 per second and this again compares favorably with the prediction of equation 4 with $C = 2$ which is 124 per second. The total event rate is 903 per second and this would suggest 8 active nucleation sites, somewhat smaller than the 14 estimated from the $3.4m/s$ data.

In contrast to the $250\mu m$ capillary, the bubbles exiting the $325\mu m$ capillary all appeared to have volumetric diameters in the range $0.5d$ to $1.2d$, with virtually no larger slugs. Perhaps there are no large slugs because there is no dominant nucleation site far enough upstream but it is otherwise hard to be sure of the reason for the difference. The typical diameter of the bubbles exiting the tube decreased with increasing flow rate, declining from about $1.0d$ at a velocity of $3m/s$ to about $0.5d$ at a velocity of $6m/s$. When the bubbles exit the capillary, they appear to be substantially distorted by the flow and may even be broken into fragments. Though the typical size changed with increasing flow rate, the rate of efflux of bubbles seemed to be independent of velocity, being about 1100 bubbles per second at all three speeds. At the three speeds examined, the tension length, l , is $3.8m$, $2.8m$ and $1.9m$ for velocities of $3m/s$, $4m/s$ and $6m/s$ respectively. Thus, while the frequency of bubble production from a single site may increase with velocity in the manner suggested by equation 4, the tension length and therefore the number of active sites may be declining so as to keep the bubble production rate constant. Using equation 4 with $C = 2$, the rate

of 1100 bubbles per second suggests that there are a total of about 8 active nucleation sites in this $325\mu\text{m}$ capillary.

We conclude that the observations of the bubbles emerging from the capillaries are consistent with the heterogeneous nucleation model. However, each capillary has its own particular number of nucleation sites and that is not capable of prediction by any current theory.

5.5 Effect of Flow Rate and Gas Concentration

With each of the capillaries, the flow rate was varied in order to determine whether nucleation preferentially occurred over one particular range of flow rates or, possibly, over some particular Reynolds number range. Even though the length, l , and therefore the surface area available for nucleation decreases with increasing velocity, a decrease in the nucleation potential was not observed experimentally perhaps because the range of flow rates over which experiments could be performed was quite limited. As mentioned earlier, the primary effect of flow rate occurred when the flow rate was increased to that value at which the internal flow became turbulent. As detailed by Creech *et al.*⁽¹⁾, over a wide range of different capillaries, gas concentrations and flow rates nucleation was often observed to occur when flow rate was increased to Reynolds numbers within the range 2000 – 3000, in other words the range at which the internal flow transitions from laminar to turbulent. Thus internal turbulence promotes nucleation. Other than the effect of internal transition, no clear influence of flow rate could be discerned.

Tests were also conducted with different gas concentrations with both O_2 and CO_2 . Since ethanolization effectively re-initialized a given capillary, it was possible to conduct repeatable tests on a particular capillary with different concentrations of both O_2 and CO_2 . In the vast majority of cases, the high concentrations of O_2 and CO_2 behaved identically in terms of whether or not nucleation occurred in a particular capillary. The most noticeable difference was that a nucleating flow with CO_2 produced higher void fractions of gas than the flow with O_2 for obvious reasons. This supports the conclusion that the dominant factor that determines whether or not macroscopic bubbles are observed is the presence or absence of nucleation sites rather than a critical concentration gradient of dissolved gas.

6. Concluding Remarks

The experiments described in this paper confirm a remarkable phenomenon in which highly-supersaturated aqueous solutions of gas may be injected through a small capillary into an aqueous environment without the formation of significant and/or

measurable gas bubbles. The experimental observations are consistent with a heterogeneous surface nucleation model put forward by Creech *et al.*⁽¹⁾. Of particular note is the estimate that, in the successful silica capillaries, the number of potential nucleation sites is of the order of ten.

It is also clear that the treatment of the interior surface of the capillary is critical to the success or failure of the objective since it can effectively eliminate those nucleation sites, though perhaps only when they are so small in number. Several treatments are remarkably effective in this regard. One simple technique that was deployed in the laboratory was to flush the capillary with ethanol after it had already been filled with an aqueous medium. Apparently, the ethanol strips out or dissolves the nucleation sites and causes them to become non-functional. This is an entirely reversible procedure; allowing the capillary to dry out re-establishes the functioning nucleation sites; and another “ethanolization” will eliminate them again. A medical device coating which has a similar though less dramatic effect is a benzalkonium heparin (BKH).

Because of the sensitivity of the phenomenon to surface treatment, each capillary is quite unique and it is therefore difficult to establish the dependence of the nucleation threshold on the fundamental flow variables, namely the capillary diameter, the flow velocity and the gas concentration. In addition, the present study established that when the flow (a) in the capillary or (b) in the emerging jet transitions from a laminar to a turbulent state this can trigger nucleation, presumably because of the greater mass transfer which occurs in the turbulent regime.

Acknowledgements

The authors are very grateful to Gustavo Joseph for his help with the high speed video observations.

References

- (1) Creech, J., Divino, V., Patterson, W., Zalesky, P.J. and Brennen, C.E., Injection of highly supersaturated oxygen solutions without nucleation, submitted for publication (2001).
- (2) Brereton, G.J., Crilly, R.J. & Spears, J.R., Nucleation in small capillary tubes, *Chemical Physics*, Vol.230 (1998), p. 253.
- (3) Brennen, C.E., *Cavitation and Bubble Dynamics*, Oxford University Press (1995).
- (4) Burkhard, M.E. & Van Liew, H.D., Simulation of exchanges of multiple gases in bubbles in the body, *Respiration Physiology*, Vol.95 (1994), p. 131-145.
- (5) Dack, M.R.J.(editor), *Solutions and solubilities*, in *Techniques of Chemistry*, Vol. VIII (1975-76), John Wiley and Sons.
- (6) Schmidt, A.X. & List, H.L., *Material and Energy Balances*, Prentice-Hall (1962).